
The Eurasia Proceedings of Science, Technology, Engineering & Mathematics (EPSTEM)

Volume 1, Pages 36-40

ICONTES2017: International Conference on Technology, Engineering and Science

QUANTITATIVE PHASE ANALYSIS OF ARMOUR STEEL WELDED JOINT BY X-RAY DIFFRACTION

Miroslav Cvetinov
University of Novi Sad

Aleksandar Čabrilo
University of Novi Sad

Katarina Gerić
University of Novi Sad

Maja Stojanović
University of Novi Sad

Olivera Klisurić
University of Novi Sad

Abstract: Ultra-high tensile strength is characteristic of armour steel and in order to preserve this strength its welding process is of paramount importance. Austenitic filler material is traditionally used for welding of armour steel, yet it has lower mechanical properties than the base material, i.e. the filler material is the weakest point of the welded joint. Moreover, due to the plastic deformation at the crack tip austenitic filler material gets transformed into martensite during fatigue crack propagation. An amount of austenite transformed into martensite is directly related to crack growth resistance in the weld metal.

In order to quantify martensite phase formed during the crack propagation under the effect of fatigue load, we employed method of X-ray diffraction. Diffractograms were recorded in Bragg-Brentano $\theta:2\theta$ reflection geometry on a Philips PW 1820/30 X-ray diffractometer employing monochromatic $\text{CuK}\alpha$ radiation (30 kV, 30 mA) in the range 40° - 60° 2θ . For the quantitative phase analysis RIR method was subsequently employed. From the obtained data, martensite to austenite ratio was calculated for the fracture surface. Thereafter the 0.05 mm thick layer was removed from specimen surface and the diffraction pattern was recorded again. This procedure was repeated till 25% of the martensite remained in two-phase mixture.

α' martensite was detected at distances up to 0.25 mm under the fracture surface. The greatest transformation of austenite into α' martensite was 55%, seen on the fracture surface. The amount of α' martensite declines with a distance by an average of $\approx 5\%/0.05$ mm, in the depth perception tests. At the distance of 0.25 mm, the amount of transformed austenite fell to 24%.

Keywords: XRD, armour steel, austenitic phase, martensite phase, welded joint, weld

Introduction

Armour steel belongs to the ultra-high tensile strength and hardness group of steels. The welding of armour steel is complicated due to the high content of carbon in the metal base and the presence of faults in the form of cracks and pores (Atabaki, Ma, Yang, & Kovacevic, 2014) in the weld metal zone, whereby fractures may be initiated in the weld metal.

- This is an Open Access article distributed under the terms of the Creative Commons Attribution-Noncommercial 4.0 Unported License, permitting all non-commercial use, distribution, and reproduction in any medium, provided the original work is properly cited.

- Selection and peer-review under responsibility of the Organizing Committee of the conference

*Corresponding author: Miroslav Cvetinov- E-mail: miroslav.cvetinov@df.uns.ac.rs

Austenitic filler material is traditionally used for welding of armour steel because of improvement of hydrogen dilution in an austenitic phase (Alkemade, 1996). This filler material has lower mechanical properties than the base material, i.e. the filler material is the weakest point of the welded joint (Magudeeswaran, Balasubramanian, & Madhusudhan, 2008). For heavy engineering structures, such as armoured military vehicles that frequently undergo impact and variable loads, mechanical properties of welded joints and the weld metal zone must be known. Due to variable loads, cracks created in the weld metal may easily propagate towards the sensitive fusion line, followed by their possible rapid growth (Shah Khan, Alkemade, Weston, & Wiese, 1998). Austenitic filler material is unstable and gets transformed into martensite during fatigue crack propagation due to plastic deformation at the crack tip (Martelo, Mateo, & Chapetti, 2015). During the metastable austenite deformation, two types of martensitic structures can be formed: ϵ – martensite with hexagonal close packed and α' – martensite, with body centered cubic crystal structure. An amount of austenite transformed into martensite is directly related to crack growth resistance in the weld metal (Mei & Morris, 1990).

In order to quantify martensite phase formed during the crack propagation under the effect of fatigue load, we employed method of X-ray diffraction.

Methods

Materials and welding process

Austenitic filler material (ASS), designated as AWS ER307, is used for welding armour steel Protac 500. Welding direction is parallel to the rolling direction. Cold rolled plates 12 mm thick are cut to the required dimensions (250 mm x 100 mm), while V joint under the angle of 55° is prepared by Water Jet Device (Figure 1.). Robot Kuka and Citronix 400A GMAW welding procedure was used during the welding process testing. Details on welding are shown in the article (Cabrilo & Geric, 2016). Robotic welding is used for human factor effect elimination, in order to allow a fine adjustment of parameters and results repeatability. Wire diameter is 1.0 mm while Figure 1. shows V joint dimensions and four - pass welding configuration.

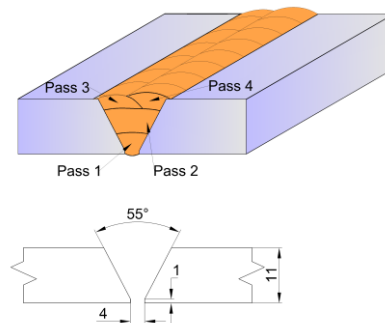


Figure 1. Schematic drawing of edge preparation and welding configuration

Fatigue Crack Growth

Three point bending specimen was used for testing. Specimens were cut by Water Jet Device, to eliminate any possibility of armour steel thermal treatment. After getting final measures in the grinding process, 5 mm long machined notch was created on specimens in the direction parallel to welding (Figure 2.), according to the E-647 standard (Annual Book of ASTM Standards, 2004). The fatigue pre-crack was inserted before the crack growth rate tests, in accordance with ASTM E-647. The length of the fatigue pre-crack was 4.7 mm. The fatigue pre-crack was realized with a high-frequency CRACTRONIC pulsator, at a load ratio $R = 0.33$, followed by a constant loading frequency of 170 Hz. Fatigue crack growth rate was tested on high-frequency CRACTRONIC pulsator, the model with force and frequency control of 145 Hz. The constant sinusoidal shape was used, while the testing was made under the load ratio $R = K_{min}/K_{max} = 0.1$.

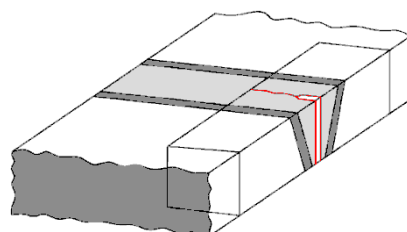


Figure 2. Specimen orientation with respect to the weld axis for fatigue crack growth test

Quantitative phase analysis by X-ray diffraction

X-ray diffraction was used to identify a martensitic transformation amount formed during the crack propagation, under the effect of fatigue load. Investigation was undertaken by X-ray diffraction in Bragg-Brentano $\theta:2\theta$ reflection geometry, at a room temperature. Diffractograms were recorded on a Philips X-ray diffractometer having a copper tube PW 1830 generator, a PW 1820 goniometer fitted with a post-diffracted graphite monochromator and a scintillation detector attached to a PW 1710 controller (30 kV, 30 mA generator settings, $\text{CuK}\alpha$ radiation). LaB_6 was used as an external standard for peak position calibration and for instrumental peak broadening assessment. XRD data were collected over the 2θ range of 40° to 60° , with a step size of 0.05° and an exposition time of 2 s per step.

From the obtained data, martensite to austenite ratio was calculated for the fracture surface. Thereafter the 0.05 mm thick layer was removed from specimen surface and the diffraction pattern was recorded again. This procedure was repeated till 25% of the martensite remained in two-phase mixture. An experimental XRD patterns decomposition (profile fitting) was performed using pseudo - Voigt function on each diffraction peak and linear function on background radiation.

For quantitative phase analysis RIR method was employed (Snyder, 1992). The RIR method scales all diffraction data to the standard. By convention, corundum is used as an international reference. The scale factor, I/I_c , was experimentally determined from the pattern strongest line ratio, I , to the corundum I_c strongest line intensity, in a 50/50 weight mixture.

To determine weight ratio of martensite and austenite in two-phase system, their scaling factors were obtained from the ICDD PDF-2 database (PDF 41293, PDF 441292, PDF 897245 and PDF 330397). Due to the heavy peak overlapping in the $43^\circ - 44.5^\circ 2\theta$ region, this method could only be employed on the second most intense peak of both martensite, $I_{2\text{mart}}$, and austenite, $I_{2\text{aust}}$, at $\sim 45.0^\circ 2\theta$ (PDF 44-1293) and $\sim 50.7^\circ 2\theta$ (Arbuzov, Golub, & Karpets, 1986, and Amar, David, Murdock, Speer, & Matlock, 2004), respectively. Intensity ratios of the two strongest lines for martensite, $(I/I_2)_{\text{mart}}$, and austenite phase, $(I/I_2)_{\text{aust}}$, were thus obtained from the same database. The following equation was used:

$$X_{\text{mart}} \cdot I_{2\text{aust}} \cdot (I/I_2)_{\text{aust}} \cdot (I/I_c)_{\text{mart}} = X_{\text{aust}} \cdot I_{2\text{mart}} \cdot (I/I_2)_{\text{mart}} \cdot (I/I_c)_{\text{aust}}$$

where $X_{\text{aust}} = 1 - X_{\text{mart}}$ and X_{mart} are weight fractions of austenite and martensite phases, respectively.

Results and Findings

Figure 3. shows the X-ray diffractograms of specimen surfaces. The diffractograms show two phases, austenite and martensite as a function of specimen thickness. Both phases have two peaks, austenite with peaks in 2θ ranges $43.2-43.6^\circ$ and $50.4-50.9^\circ$, and martensite with its peaks at $43.5-44.2^\circ$, 44.8° and 45.0° .

The most intense peaks of α' martensite and austenite overlap not only in our specimen, but in other alloy steels published in ICDD PDF-2. The uncertainty inherent in deconvolution of heavily overlapping peaks, makes them unsuitable for weight ratio determination. Therefore, the second most intense peaks were used. These peaks are only twice less intense than their stronger counterparts and therefore absolutely sufficient for precise weight ratio calculation.

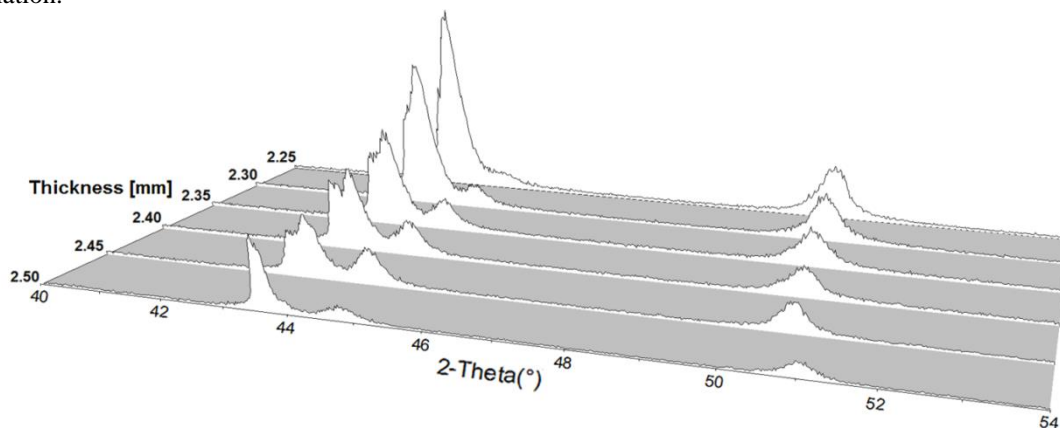


Figure 3. XRD Diffractograms of specimens under investigation

Since higher surface roughness causes increased diffuse X-ray scattering, peak intensities inversely correlate with the thickness of the specimens under investigation. Nevertheless, using the RIR method (reference intensity ratio), the ratio of integrated intensities of α' martensite and austenite diffraction peaks reliably indicates their weight ratio in surface layers.

Table 1 shows a changes percentage per level in relation to the fracture surface. α' martensite was detected at distances up to 0.25 mm under the fracture surface. The greatest transformation of austenite into α' martensite was 55%, seen on the fracture surface. The amount of α' martensite declines with a distance by an average of $\approx 5\%/0.05$ mm, in the depth perception tests. At the distance of 0.25 mm, the amount of transformed austenite fell to 24%.

Table 1. α' - Martensite weight fractions vs. specimen thickness

Specimen thickness	[mm]	2.50	2.45	2.4	2.35	2.30	2.25
α' - Martensite weight	[%]	55	50	46	34	30	24
Tolerance	[%]	± 3	± 3	± 2	± 2	± 2	± 2

Conclusion

It is known that welded joints are very heterogeneous, since they include weld metal and base metal. The base metal in welded joints of armour steel is always of higher hardness than the weld metal. This work examined welded joints with four passes.

Formation of fatigue induced fracture depends on external factors such as load and internal factors such as mechanical properties of the material and its microstructure. It is known that in stainless steel, being metastable materials, austenite transformation into martensite may occur during a fatigue crack growth; this is the result of intensive plastic deformation at the crack tip. Phase transformations taking place at the crack tip (Nakajima, Akita, Uematsuc, & Tokaji, 2010) decrease the crack growth rate in the linear region (Grujicic, Lai, & Gumbsch, 1997). Martensitic transformation takes place only in the thin layer close to the fracture surface and in these steels it causes an increase in volume (Haušild, Davydov, Drahoukoupil, Landa, & Pilvin, 2010).

X-ray diffraction ascertained the direct transformation of γ - austenite into α' - martensite in austenitic filler material AWS 307.

Acknowledgements

This study was financially supported by the Ministry of Education, Science and Technological Development of the Republic of Serbia through the grants no. ON 174004. and no. OI171015.

References

- Alkemade S.J., (1996). *The Weld Cracking Susceptibility of High Hardness Armour Steel*. Australia.
- Amar K.D., David C., Murdock C.M., Speer J.G., & Matlock K.D. (2004). Quantitative measurement of deformation-induced martensite in 304 stainless steel by X-ray diffraction. *Scripta Materialia*. 50, 1445-1449.
- Annual Book of ASTM Standards, Volume 03.01. (2004). *ASTM E647-08: Standard test method for measurement of fatigue crack growth rates*. West Conshohocken, PA: ASM International.
- Atabaki M.M., Ma J., Yang G., & Kovacevic R. (2014). Hybrid laser/arc welding of advanced high strength steel in different butt joint configurations. *Materials and Design*. 64, 573–587.
- Arbuzov M., Golub S.Y., & Karpets M. (1986). Structure of austenite ordering in chromium steels. *Fizika Metallov i Metallovedenie*. 62, 108-111.
- Cabrilo A., & Geric K. (2016). Weldability of High hardness armour steel. *Advanced Materials Research*. 1138, 79-84.
- Grujicic M., Lai S.G., & Gumbsch P. (1997), Atomistic simulation study of the effect of martensitic transformation volume change on crack-tip material evolution and fracture toughness. *Materials Science and Engineering A*. 231, 151–162.
- Haušild P., Davydov V., Drahoukoupil J., Landa M., & Pilvin P. (2010). Characterization of strain-induced martensitic transformation in a metastable austenitic stainless steel. *Materials and Design*. 31, 1821–1827.

- Magudeeswaran G., Balasubramanian V., & Madhusudhan R.G. (2008). Effect of welding processes and consumables on high cycle fatigue life of high strength, quenched and tempered joints. *Materials and Design*. 29, 1821-1827.
- Martelo D.F., Mateo A., & Chapetti M. D. (2015). Crack closure and fatigue crack growth near threshold of a metastable austenitic stainless steel, *International Journal of Fatigue*. 77, 64–77.
- Mei Z., & Morris J.W. (1990). Influence of deformation-induced martensite on fatigue crack propagation in 304-type steels. *Metallurgical and Materials Transaction A*. 12(21), 3137–52.
- Nakajima M., Akita M., Uematsuc Y., & Tokaji K. (2010). Effect of strain-induced martensitic transformation on fatigue behavior of type 304 stainless steel. *Procedia Engineering*. 2, 323–330.
- Shah Khan M.Z., Alkemade S.J., Weston G.M., & Wiese D.G. (1998). Variable-amplitude fatigue testing of a high hardness armour steel. *International Journal of Fatigue*. 3(20), 233-239.
- Snyder R.L. (1992). The Use of Reference Intensity Ratios in X-Ray Quantitative Analysis. *Powder Diffraction*. 7, 186-193.